Head and Neck Pathology (2023) 17:393–400
https://doi.org/10.1007/s12105-022-01513-x

ORIGINAL PAPER

A Subset of Salivary Intercalated Duct Lesions Harbors Recurrent *CTNNB1* and *HRAS* Mutations: A Molecular Link to Basal Cell Adenoma and Epithelial-Myoepithelial Carcinoma?

Anne C. McLean[1] · Lisa M. Rooper[2] · Jeffrey Gagan[1] · Lester D. R. Thompson[3] · Justin A. Bishop[1]

Received: 12 November 2022 / Accepted: 22 November 2022 / Published online: 8 December 2022

Abstract

Background Intercalated duct lesions (IDLs) are benign salivary gland proliferations that resemble normal intercalated ducts and are subdivided into hyperplastic, adenoma or hybrid types depending on circumscription. While IDLs were historically regarded as non-neoplastic, frequent association with basal cell adenoma (BCA) and epithelial-myoepithelial carcinoma (EMC) has raised the possibility that they are neoplastic precursors.

Methods In this study, we performed β-catenin immunohistochemistry and targeted molecular analysis on IDLs to clarify their pathogenesis.

Results We identified 15 IDLs from the parotid glands of eight men and six women with a median age of 65 years (range 42–85 years). These lesions included nine hyperplastic, three adenoma, and three hybrid types. Nuclear β-catenin localization was present in 7 of 13 lesions tested (54%). Next generation sequencing was successfully completed in 12 IDLs, of which seven (58%) had likely oncogenic mutations. These included three recurrent *CTNNB1* mutations in hyperplastic ($n=2$) and hybrid ($n=1$) lesions and two recurrent *HRAS* hotspot mutations in adenomas.

Conclusion Despite substantial heterogeneity, these findings confirm that a majority of IDLs are genuinely neoplastic, and some demonstrate molecular overlap with both BCA and EMC, supporting their theorized role as precursors to these tumors. Nevertheless, no oncogenic drivers were present in a significant subset of cases, suggesting that some IDLs may be truly reactive and hyperplastic. As such, IDL appear to represent a diverse morphologic and molecular spectrum that include both neoplastic and hyperplastic lesions. Reconsideration of the boundary between IDL and BCA in the future may be necessary to simplify classification.

Keywords Salivary glands · Intercalated duct lesion · Intercalated duct hyperplasia · Intercalated duct adenoma · Molecular diagnostics

Introduction

Intercalated duct lesions (IDLs) of the salivary glands are benign epithelial proliferations that show close histologic resemblance to normal intercalated ducts [1–4]. They are subdivided into hyperplasia and adenoma categories based on their degree of circumscription and encapsulation, with rare hybrid cases that show overlapping features [5–7]. However, the etiology of IDLs remains ambiguous. Because they tend to be very small and are generally found incidentally in salivary glands resected for other pathologies [6], IDLs have historically been regarded as a reactive/hyperplastic process—a conception reflected in their classification as non-neoplastic under the term intercalated duct hyperplasia in the 4th edition WHO Classification of Head and Neck

Anne C. McLean and Lisa M. Rooper have contributed equally to this work.

✉ Justin A. Bishop
Justin.Bishop@UTSouthwestern.edu

[1] Department of Pathology, University of Texas Southwestern Medical Center, 6201 Harry Hines Blvd Room UH04.250, Dallas, TX 75390, USA

[2] Department of Pathology, The Johns Hopkins Hospital, Baltimore, MD, USA

[3] Head and Neck Pathology Consultations, Woodland Hills, CA, USA

Tumours [8, 9]. However, IDLs are commonly associated with or even transition into basal cell adenoma (BCA) and epithelial-myoepithelial carcinoma (EMC), and frequently show nuclear localization of β-catenin, raising the possibility that they represent a neoplastic process [2–4, 10–20]. The fifth edition WHO Classification of Head and Neck Tumours has categorized both intercalated duct hyperplasia and intercalated duct adenoma as benign neoplasms [21]. Nevertheless, the neoplastic nature of IDL has not yet been definitively established, and it is still not entirely certain whether the subsets designated as hyperplasia and adenoma even represent the same entity.

Recently, molecular analysis has substantially clarified the pathogenesis of various benign and malignant salivary gland tumors. Identification of recurrent fusions or point mutations across the spectrum of salivary gland pathology has allowed for definition of new tumor types, clarified the boundaries of longstanding entities, and cemented relationships between various neoplasms [7, 22–26]. Notably, the salivary gland tumors most frequently associated with IDL both have a distinctive and well-established molecular profile. Up to 80% of BCA harbor recurrent *CTNNB1* mutations [27–30]. Furthermore, up to 78% of EMCs that arise independent of pleomorphic adenoma demonstrate *HRAS* mutations [31–33]. However, IDLs have never been thoroughly investigated at the molecular level. In this study we performed next generation sequencing on a series of IDL including all morphologic subtypes to better characterize their pathogenesis and relationships to other salivary gland entities.

Materials and Methods

Case Selection

Cases of IDL were retrieved from the authors' surgical pathology archives and consultation files. Similar to criteria previously described by Weinreb, et al. [3] we defined cases as IDL and selected them for inclusion in this study if they: (1) included a proliferation of small tubules composed of a biphasic population of cuboidal ductal cells and attenuated myoepithelial cells resembling normal intercalated ducts, (2) had a diameter of at least 1 mm, and (3) lacked inflammation and atrophy of surrounding salivary gland tissue. In all cases, the assessment of the biphasic nature of the lesions was evident on hematoxylin and eosin alone and no confirmatory immunohistochemistry was necessary. We included IDLs that were found incidentally during resection of salivary gland neoplasms or in neck dissections for head and neck cancer as well as those that were recognized clinically and were the primary targets of surgical intervention. However, IDLs that showed direct transition into another tumor type were excluded. All available sections from each case were reviewed by the authors, and their histologic features recorded. All available clinical information for each patient was collected from the electronic medical record.

We also classified all IDLs as hyperplastic, adenoma, or hybrid types based on a modification of the features described in the fifth edition WHO classification and by Weinreb, et al. [3, 21]. Hyperplastic IDLs were non-encapsulated with imperceptible blending between the intercalated duct proliferation and surrounding acinar tissue. Adenomas were encapsulated or well-circumscribed and lacked close admixture of salivary acini with the duct proliferation. Hybrid IDLs showed both non-encapsulated and encapsulated/well-circumscribed areas.

Immunohistochemistry

Immunohistochemistry for β-catenin was performed on all cases using a mouse monoclonal antibody against β-catenin (Sigma-Aldrich, St. Louis, MO). Five-micron sections of formalin-fixed, paraffin-embedded tissue were cut, deparaffinized, and subjected to antigen retrieval using 10 mM citrate buffer at 92 °C for 30 min. Immunohistochemical signals were visualized using the Ultra view polymer detection kit (Ventana Medical Systems, Inc. Tucson, AZ) on a Ventana Benchmark Ultra autostainer (Ventana Medical Systems). Staining was performed according to manufacturer's instructions in the presence of appropriate controls. β-catenin was interpreted as positive if 10% or more of the nuclei in the abluminal layer showed nuclear localization of staining.

Next-Generation Sequencing

Targeted next generation sequencing was performed on all IDL as described in detail previously [34]. Briefly, unstained slides were cut at five-μm thickness from formalin-fixed, paraffin-embedded tissue blocks, and the IDLs were microdissected for analysis. DNA was isolated using Qiagen AllPrep kits (Qiagen, Germantown, MD), and an enriched library containing all exons from > 1,505 cancer-related genes was created using custom NimbleGen probes (Roche, Indianapolis, IN). Sequencing was performed on a NextSeq 550 (Illumina, San Diego, CA) with a median 900 × target exon coverage. Variants were reviewed using the Integrated Genomics Viewer (Broad Institute, Cambridge, MA) and annotated using the gnomAD and dbSNP databases.

Results

Clinical Findings

Clinical and demographic data are presented in Table 1. We identified fifteen IDLs representing fourteen patients

including eight men and six women (male: female ratio 1.3:1). Patients had a median age of 65 years (range 42–85 years). While thirteen patients had a solitary IDL, one patient had two separate lesions. All IDLs arose in the parotid gland. Nine patients had IDL found incidentally in specimens taken for other pathology, including seven with separate salivary gland tumors and two in neck dissections necessitated by other head and neck malignancies, whereas five had parotidectomies performed for resection of the IDL itself. The IDLs had a median size of 3 mm overall (range 1–15 mm), although the subset of cases recognized clinically had a higher median size of 12 mm (range 5–15 mm).

Histologic Findings

All fifteen IDLs fell within the previously reported histologic spectrum of this entity. They consisted of closely packed, back-to-back tubular proliferations of intercalated ducts composed of cuboidal to columnar epithelial cells with homogenous eosinophilic to focally clear cytoplasm (Fig. 1A). A single layer of attenuated abluminal myoepithelial cells were consistently present surrounding the ductal formations (Fig. 1B). No cytologic atypia, necrosis, or increased mitoses were observed, and the surrounding glandular tissue was uninflamed and lacked atrophic changes. Nine of the IDLs (60%) had hyperplastic morphology. These lesions were completely unencapsulated (Fig. 1C) and had edges that interdigitated gradually into surrounding parotid gland parenchyma, with scattered acinar units intermixed at the periphery (Fig. 1D). Three IDLs (20%) were classified as adenomas. They were thickly encapsulated and entirely demarcated from surrounding parotid parenchyma without intermixed acinar cells (Fig. 1E). The final three IDLs (20%) were hybrid lesions. This group included both adenomatous areas that were clearly delineated and thinly encapsulated, and more hyperplastic zones that blended into the surrounding salivary parenchyma and fat (Fig. 1F).

All IDLs were spatially separated from any other salivary gland tumor in the specimen, with no cases that showed transition between the IDL and accompanying adenoma or carcinoma. A total of four different salivary gland tumor types were seen in association with IDLs. The most common tumor type seen was EMC in three cases (21%), one of which was an apocrine subtype and one of which arose ex-pleomorphic adenoma. There were also benign pleomorphic adenomas in two cases (14%), BCA in one case (7%), and myoepithelioma in one case (7%). The IDL associated with the other salivary tumors included seven hyperplastic lesions and one adenoma. Hyperplastic IDLs were also incidentally identified in two patients undergoing neck dissection for squamous cell carcinoma and papillary thyroid carcinoma. IDLs that presented as clinically recognizable nodules without accompanying salivary or neck pathology included three hybrid lesions and two adenomas.

Table 1 Clinical and demographic information

Case	Age (years)	Sex	Site	Reason for surgery	Size (mm)	Histologic type	Beta-catenin IHC	Oncogenic mutation (VAF)
1	81	M	Parotid gland	EMC	6	Adenoma	+	VUS
2	48	F	Parotid gland	EMC with apocrine IDC	4	Hyperplastic	+	*CTNNB1* p.I35T (11.19%)
3	85	F	Parotid gland	BCA	3	Hyperplastic	+	*CTNNB1* p.I35T (11.43%)
4	74	M	Parotid gland	EMC ex-PA	1	Hyperplastic	–	VUS
5	64	F	Parotid gland	PA	1.5	Hyperplastic	–	NA
6	79	M	Parotid gland	Neck dissection for SCC	2	Hyperplastic	+	VUS
7	74	M	Parotid gland	Neck dissection for PTC	1.5	Hyperplastic	–	NA
8	60	M	Parotid gland	PA	3	Hyperplastic	NA	VUS
9	42	F	Parotid gland	IDL identified clinically	12	Hybrid	+	*CTNNB1* p.I35T (15.12%)
10	59	M	Parotid gland	Myoepithelioma	1 and 1.5	Hyperplastic × 2	+*	*NRAS* p.Q61H (1.79%)*
11	56	M	Parotid gland	IDL identified clinically	15	Hybrid	+	VUS
12	44	F	Parotid gland	IDL identified clinically	7	Hybrid	–	*MDM2* 12-copy amplification
13	73	M	Parotid gland	IDL identified clinically	10	Adenoma	–	*HRAS* p.Q61R (9.69%)
14	72	F	Parotid gland	IDL identified clinically	5	Adenoma	–	*HRAS* p.Q61K (9.35%), *VHL* p.R69C (5.86%)

M male, *F* female, *BCA* basal cell adenoma, *EMC* epithelial-myoepithelial carcinoma, *IDC* intraductal carcinoma, *IDL* intercalated duct lesion, *IHC* immunohistochemistry, *NA* not available, *PA* pleomorphic adenoma, *PTC* papillary thyroid carcinoma, *SCC* squamous cell carcinoma, *VAF* variant allele fraction, *VUS* variant(s) of uncertain significance

*Both IHC and next-generation sequencing were only performed on the largest of the two IDLs in this case

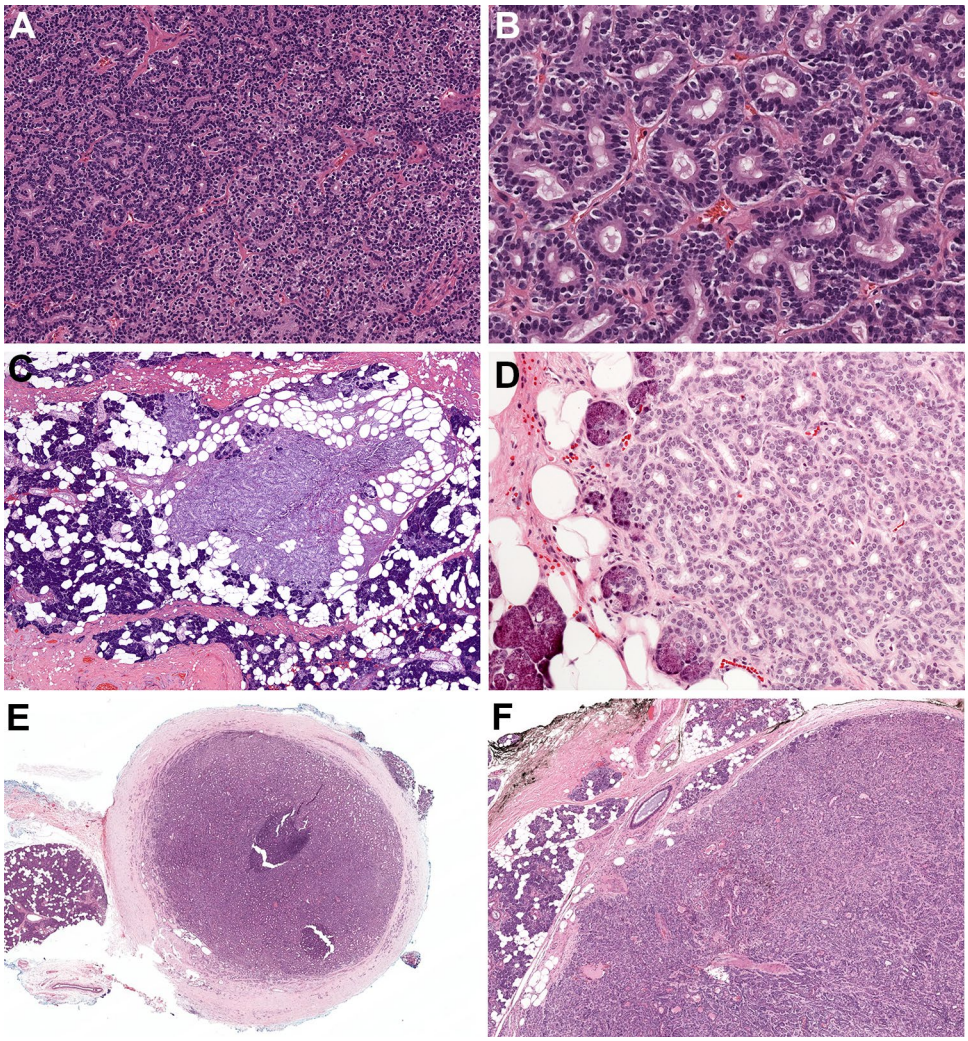

Fig. 1 The IDLs were composed of back-to-back tubules and ducts composed of cuboidal to columnar epithelial cells with homogenous eosinophilic cytoplasm (**A**, 10x). A single layer of attenuated myoepithelial cells surrounded the central ducts (**B**, 20x). Hyperplastic lesions were unencapsulated and interdigitated with surrounding parotid gland parenchyma (**C**, 4x), merging with acini at the periphery (**D**, 20x). Adenomas had a well-defined capsule throughout (**E**, 2x). Hybrid lesions included both encapsulated and non-encapsulated areas (**F**, 4x)

Immunohistochemical Findings

β-catenin immunohistochemistry was successfully performed in thirteen IDL, with tissue lost in processing in one case and only the largest lesion stained in the case with two IDL. Overall, seven cases (54%) demonstrated nuclear positivity for β-catenin in at least 10% of the abluminal cells, identical to the pattern that is seen in BCA (Fig. 2A). This group included four hyperplastic IDLs (57%, Fig. 1D), one adenoma (33%, Fig. 2C), and two hybrid IDLs (66%, Fig. 3C). The remaining IDLs showed no nuclear localization of β-catenin (Fig. 2B).

Molecular Findings

Molecular results are summarized in Fig. 3. Next-generation sequencing was successfully completed in twelve IDLs; one case failed quality assurance, one had lesional tissue depleted, and only the largest lesion was tested in the case with two IDLs. Overall, seven IDLs (58%) displayed likely oncogenic mutations. The most common alterations identified were *CTNNB1* p.I35T mutations in three cases (25%) and hotspot *HRAS* p.Q61K and p.Q61R mutations in two cases (17%). One case with *HRAS* mutation also showed a likely oncogenic *VHL* p.R69C mutation. One additional case each (8%) displayed likely oncogenic *NRAS* p.Q61H mutation and *MDM2* 12-copy amplification. The remaining five cases harbored only variants of uncertain significance in genes known to be involved in cancer.

The seven IDLs with likely oncogenic mutations included three hyperplastic lesions (50%), two hybrid lesions (67%) and two adenomas (67%). The three *CTNNB1* mutations were seen in two hyperplastic and one hybrid lesion, both *HRAS* mutations were identified in adenomas, the one case with *MDM2* amplification was a hybrid lesion, and the single *NRAS* mutation was present in a hyperplastic lesion. Overall, although all three tumors with *CTNNB1* mutations did show corresponding nuclear localization of β-catenin, these cases represented only 43% of IDL with β-catenin positivity that were sequenced. However, the hyperplastic

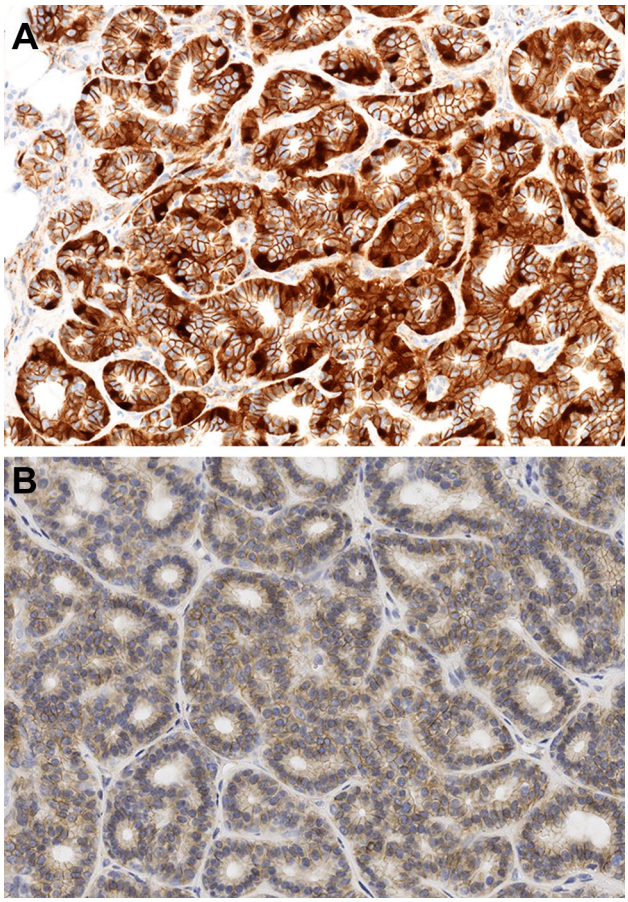

Fig. 2 Seven IDLs demonstrated nuclear localization of β-catenin in a subset of the abluminal cells, similar to BCA (**A**, 20x), while six IDLs lacked nuclear β-catenin (**B**, 20x)

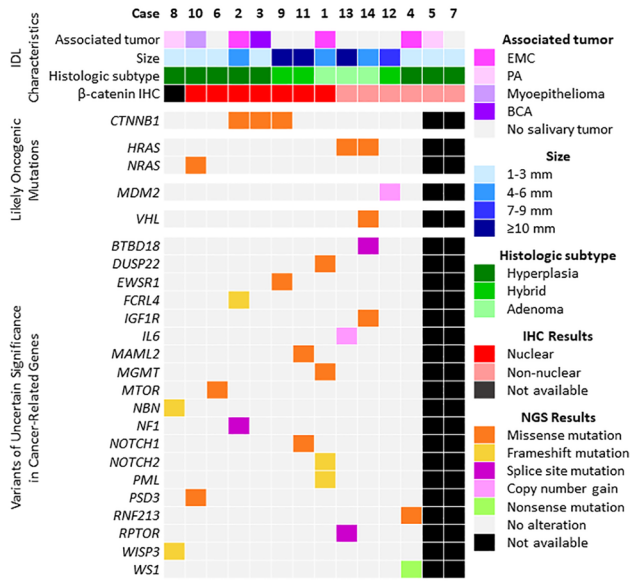

Fig. 3 Clinical, histologic, immunohistochemical, and molecular features of IDL are depicted with cases organized by molecular findings. Recurrent likely oncogenic mutations were identified in *CTNNB1* in two hyperplastic and one hybrid lesions, all of which showed nuclear β-catenin expression, and *HRAS* in two adenomas that were β-catenin negative

IDL with *NRAS* mutation at a very low allele frequency of 1.79% also had nuclear β-catenin. The tumors with *HRAS* mutation and *MDM2* amplification lacked β-catenin expression. No clear association between molecular profile and accompanying salivary tumors was noted, with only one IDL with *CTNNB1* mutation arising in a salivary gland removed for basal cell adenoma.

Discussion

Salivary IDLs have been acknowledged in the literature for nearly 30 years using a variety of terms. Although the 4th edition WHO Classification of Head and Neck Tumours classified them as an exclusively non-neoplastic process under the name intercalated duct hyperplasia [8], the fifth edition recognizes both intercalated duct hyperplasia and intercalated duct adenoma as benign neoplasms [21]. However, the true nature of IDLs remains somewhat enigmatic, and it is not yet clear whether they should all be regarded as neoplastic—or even whether IDL classified as hyperplastic, adenoma, or hybrid lesions truly represent the same entity. Despite widespread application of molecular testing to reclassify many existing salivary tumors and define new tumor types, the molecular underpinnings of IDL have never been fully investigated. In this study, we performed next generation sequencing on a cohort of IDLs to better understand their pathogenesis and relationships with other entities.

First, these findings provide molecular confirmation that a subset of IDL are neoplastic and represent a precursor of BCA. Historically, several overlapping features have led to increasing consensus that there is a relationship between IDL and BCA. Not only is BCA the most common salivary gland neoplasm seen in association with IDL, but a consistent subset of cases show overt histologic transition between these lesions [3, 14]. IDLs also display some histologic similarities to BCA, including biphasic ductal and myoepithelial cell populations, frequent tubular architecture, and occasional accumulation of basement membrane material [3, 14]. Moreover, the majority of IDLs demonstrate immunohistochemical positivity for β-catenin that parallels the staining seen in BCA [14]. The presence of *CTNNB1* mutations in three IDLs in this study, in combination with one case reported previously, not only confirms their neoplastic nature but adds a layer of molecular overlap with BCA [17, 27–30]. In the setting of the many other similarities between these entities, these molecular results cement the status of IDL as a BCA precursor.

Additionally, these results raise the possibility that a separate subset of IDLs might be precursors of EMC. Although the association of EMC and IDL is less well-substantiated than that of BCA, speculation about a relationship between these entities has persisted since the initial description of IDL. Aside from BCA, EMC are the tumor most frequently found adjacent to IDL, and rare cases displaying transition from IDL to EMC have been reported in the literature [2, 12]. Additionally, many of the same morphologic features that raise parallels between IDL and BCA also overlap with EMC, including biphasic ductal and myoepithelial populations and tubular architecture. In this study, two adenoma-type IDLs demonstrated *HRAS* mutations, analogous to those recurrently identified in EMC [31–33]. Of course, *HRAS* mutations are not entirely specific to EMC in the salivary glands, as they can also be seen in a subset of other tumors including salivary duct carcinoma and apocrine intraductal carcinoma [35–37]. As such, it is possible that these adenomatous lesions represent an entirely separate benign salivary gland neoplasm that also happens to have *HRAS* mutations. However, given the other associations between IDL and EMC, this molecular overlap suggests that IDLs may also represent an EMC precursor.

Interestingly however, neither *CTNNB1* nor *HRAS* mutations are a uniform feature of IDL—even those with nuclear β-catenin localization. Two lesions had alternate likely oncogenic findings, including *MDM2* amplification and *NRAS* mutation. As neither BCA nor EMC has an entirely uniform molecular profile, IDLs with other mutations could still represent precursors to these tumors. Moreover, the presence of any oncogenic alterations does corroborate the neoplastic nature of a subset of IDLs. However, 42% of IDLs in this study lacked known oncogenic drivers, and only 43% of IDL with nuclear β-catenin harbored *CTNNB1* mutations. One likely explanation for these findings is technical. Most IDLs with discrepant β-catenin and *CTNNB1* status measured 1–3 mm, making it possible that *CTNNB1* mutations were present at a level too low for detection in these very small lesions. Indeed, one of these IDLs had *NRAS* mutation at an extremely low variant allele fraction of 1.79%, suggesting that other alterations could have been undetectable. However, other IDLs with nuclear β-catenin expression were 6 and 15 mm, respectively, making it less likely that a significant mutation was missed due to cellularity in all cases. Furthermore, at least one IDL lacked either nuclear β-catenin or likely oncogenic mutations. Therefore, it remains possible that some IDLs represent truly hyperplastic processes. While it is currently premature to regard all IDLs as neoplasms, sequencing larger numbers of cases or applying other techniques such as global methylation profiling will be necessary to definitively determine their pathogenesis.

Despite the possibility that IDL may include both hyperplastic and neoplastic lesions, histologic separation into hyperplasia, adenoma, and hybrid categories does not appear to fully delineate these etiologies. There is some correlation between morphologic patterns and molecular findings in IDL, with *CTNNB1* mutations seen only in hyperplastic and hybrid IDLs and *HRAS* mutations exclusively occurring in adenomas. Nuclear β-catenin localization was also seen in 63% of hyperplastic and 67% of hybrid IDLs compared to just 33% of adenomas. Nevertheless, the overall frequency of likely oncogenic alterations did not differ widely between groups, with 67% of the adenoma and hybrid lesions and 50% of hyperplastic lesions demonstrating driver mutations despite the potential confounding effect of lesion size in the hyperplasia group. Furthermore, there were undeniable morphologic similarities across all categories, and hybrid lesions indicated a possible transition state between hyperplastic lesions and adenomas. As such, IDLs may represent a spectrum rather than discrete categories.

In light of the apparent spectrum within the boundaries of IDL, our findings also raise the question of how to best separate IDL and BCA. Studies that described lesions transitioning from IDL to BCA noted several histologic differences between the components, with BCA showing larger and more basaloid cells, a multilayered abluminal population, attenuated lumina, and more abundant stroma [7, 14, 15]. This study by definition excluded lesions with overt IDL and BCA elements. Nevertheless, these distinctions are relatively subtle, and we find it difficult to rely on them to separate IDL and BCA given their other morphologic, immunohistochemical, and molecular similarities. In particular, differentiation of IDL from BCA becomes murky in lesions with a partial or complete capsule. Indeed, we wonder if intercalated duct adenomas might better be simply regarded as small BCAs—and hybrid lesions as IDLs undergoing transition to BCA. Under such a concept, encapsulation could easily distinguish IDL and BCA without requiring more subtle histologic judgments, leaving entirely unencapsulated hyperplastic-type lesions as the true IDL. The best classification of adenomas with *HRAS* mutations would need further investigation under such a definition. Of course, this question is admittedly academic in these benign lesions—the critical issue at the junction between IDL and BCA lays in not mistaking irregular borders for invasion and erroneous classification as basal cell adenocarcinoma. However, the distinction between these entities should be further considered to facilitate the best classification.

In summary, the molecular underpinnings of IDL are somewhat heterogeneous in this small cohort. However, we identified oncogenic mutations in 58% of IDLs, including recurrent *CTNNB1* activation that correlates with β-catenin nuclear overexpression in a subset of hyperplastic and hybrid lesions and *HRAS* mutations in a majority of adenomas. These findings provide molecular support to corroborate extensive histologic and immunohistochemical evidence that

IDLs are precursors to BCA and also suggest a close link with EMC. Nevertheless, a significant subset of IDLs lacked oncogenic drivers, raising the possibility that this category also encompasses some truly hyperplastic lesions. Despite partial correlation between molecular findings and morphology, there appears to be overlap across hyperplasia, hybrid, and adenoma subtypes, suggesting that these groups of IDLs comprise a spectrum rather than entirely separate entities and raising additional questions about where to best draw the line between IDL and BCA. Further characterization of larger groups of IDLs and exploration of their relationships with BCA and EMC should allow for better understanding of their pathogenesis in the future.

Author Contributions ACM, LMR, and JAB designed the study, performed data collection and interpretation, and prepared the manuscript. LDRT and JG performed data collection and interpretation. All authors read and approved the final paper.

Funding This study was funded by the Jane B. and Edwin P. Jenevein M.D Endowment for Pathology at UT Southwestern Medical Center. No external funding was obtained for this study.

Data Availability All data generated or analyzed during this study are included in this published article.

Code Availability Not applicable.

Declarations

Conflict of interest All authors certify that they have no affiliations with or involvement in any organization or entity with any financial interest or non-financial interest in the subject matter or materials discussed in this manuscript.

Ethical Approval All procedures performed in this retrospective data analysis involving human participants were in accordance with the ethical standards of the institutional review board (UT Southwestern IRB 112017–073).

Consent to Participate/Publication The IRB-approved study did not require informed consent.

References

1. Tandler B, Nagato T, Toyoshima K, Phillips CJ. Comparative ultrastructure of intercalated ducts in major salivary glands: a review. Anat Rec. 1998;252(1):64–91.
2. Di Palma S. Epithelial-myoepithelial carcinoma with co-existing multifocal intercalated duct hyperplasia of the parotid gland. Histopathology. 1994;25(5):494–6.
3. Weinreb I, Seethala RR, Hunt JL, Chetty R, Dardick I, Perez-Ordonez B. Intercalated duct lesions of salivary gland: a morphologic spectrum from hyperplasia to adenoma. Am J Surg Pathol. 2009;33(9):1322–9.
4. Yu GY, Donath K. Adenomatous ductal proliferation of the salivary gland. Oral Surg Oral Med Oral Pathol Oral Radiol Endod. 2001;91(2):215–21.
5. Mok Y, Pang YH, Teh M, Petersson F. Hybrid intercalated duct lesion of the parotid: diagnostic challenges of a recently described entity with fine needle aspiration findings. Head Neck Pathol. 2016;10(2):269–74.
6. Berdugo J, Chiosea S, Peel R, Berg A, Seethala RR. Salivary intercalated duct lesions: a single institution prospective study of 230 totally submitted superficial parotid glands. Mod Pathol. 2018;31.
7. Weinreb I, Zhang L, Tirunagari LM, Sung YS, Chen CL, Perez-Ordonez B, et al. Novel PRKD gene rearrangements and variant fusions in cribriform adenocarcinoma of salivary gland origin. Genes Chromosomes Cancer. 2014;53(10):845–56.
8. Chiosea S, Seethala R, Williams MD. Intercalated duct hyperplasia. In: El-Naggar A, Chan JK, Grandis JR, Takata T, Slootweg PJ, editors. WHO classification of head and neck tumours. Lyon, France: International Agency for Research on Cancer; 2017. p. 197.
9. Seethala RR, Stenman G. Update from the 4th edition of the World Health Organization classification of head and neck tumours: tumors of the salivary gland. Head Neck Pathol. 2017;11(1):55–67.
10. Adhikari BR, Nishimura M, Takimoto K, Harada F, Onishi A, Hiraki D, et al. Adenomatous ductal proliferation/hyperplasia in the parotid gland associated without any other pathological lesions; a report and survey of the literatures. Med Mol Morphol. 2018;51(4):244–8.
11. Bilodeau EA, Acquafondata M, Barnes EL, Seethala RR. A comparative analysis of LEF-1 in odontogenic and salivary tumors. Hum Pathol. 2015;46(2):255–9.
12. Chetty R. Intercalated duct hyperplasia: possible relationship to epithelial-myoepithelial carcinoma and hybrid tumours of salivary gland. Histopathology. 2000;37(3):260–3.
13. Luna MA. Salivary gland hyperplasia. Adv Anat Pathol. 2002;9(4):251–5.
14. Magliocca KR, Seethala RR. Salivary intercalated duct lesions in transition. Histopathology. 2016;69(4):710–1.
15. Montalli VA, Martinez E, Tincani A, Martins A, Abreu Mdo C, Neves C, et al. Tubular variant of basal cell adenoma shares immunophenotypical features with normal intercalated ducts and is closely related to intercalated duct lesions of salivary gland. Histopathology. 2014;64(6):880–9.
16. Seki N, Yamazaki N, Ikeda T, Hadara H, Himi T. A symptomatic case of adenomatous ductal proliferation/hyperplasia with a large cystic lesion. Case Rep Oncol. 2017;10(2):676–82.
17. Kusafuka K, Baba S, Kitani Y, Hirata K, Murakami A, Muramatsu A, et al. A symptomatic intercalated duct lesion of the parotid gland: a case report with immunohistochemical and genetic analyses. Med Mol Morphol. 2022. https://doi.org/10.1007/s00795-022-00328-7.
18. Ohtomo R, Mori T, Shibata S, Tsuta K, Maeshima AM, Akazawa C, et al. SOX10 is a novel marker of acinus and intercalated duct differentiation in salivary gland tumors: a clue to the histogenesis for tumor diagnosis. Mod Pathol. 2013;26(8):1041–50.
19. Li B, Jie W, He H. Myb immunohistochemical staining and fluorescence in situ hybridization in salivary rare basaloid lesions. Front Oncol. 2020;10:870.
20. Chenevert J, Duvvuri U, Chiosea S, Dacic S, Cieply K, Kim J, et al. DOG1: a novel marker of salivary acinar and intercalated duct differentiation. Mod Pathol. 2012;25(7):919–29.
21. Chiosea S, Di Palma S, Thompson LDR, Weinreb I, Williams MD. Intercalated duct adenoma and hyperplasia. In *WHO classification of head and neck tumours*, WHO Classification of Tumours Editorial Board (ed.). Lyon, France: International Agency for Research on Cancer, 2022.
22. Agaimy A, Ihrler S, Baneckova M, Costes Martineau V, Mantsopoulos K, Hartmann A, et al. HMGA2-WIF1 rearrangements

characterize a distinctive subset of salivary pleomorphic adenomas with prominent trabecular (canalicular adenoma-like) morphology. Am J Surg Pathol. 2022;46(2):190–9.
23. Bishop JA, Weinreb I, Swanson D, Westra WH, Qureshi HS, Sciubba J, et al. Microsecretory adenocarcinoma: a novel salivary gland tumor characterized by a recurrent MEF2C-SS18 Fusion. Am J Surg Pathol. 2019;43(8):1023–32.
24. Chiosea SI, Dacic S, Nikiforova MN, Seethala RR. Prospective testing of mucoepidermoid carcinoma for the MAML2 translocation: clinical implications. Laryngoscope. 2012;122(8):1690–4.
25. Rooper LM, Argyris PP, Thompson LDR, Gagan J, Westra WH, Jordan RC, et al. Salivary mucinous adenocarcinoma is a histologically diverse single entity with recurrent AKT1 E17K mutations: clinicopathologic and molecular characterization with proposal for a unified classification. Am J Surg Pathol. 2021;45(10):1337–47.
26. Weinreb I, Hahn E, Dickson BC, Rooper LM, Rupp NJ, Freiberger SN, et al. Microcribriform adenocarcinoma of salivary glands: a unique tumor entity characterized by an SS18::ZBTB7A fusion. Am J Surg Pathol. 2022. https://doi.org/10.1097/PAS.0000000000001980.
27. Jo VY, Sholl LM, Krane JF. Distinctive patterns of ctnnb1 (beta-catenin) alterations in salivary gland basal cell adenoma and basal cell adenocarcinoma. Am J Surg Pathol. 2016;40(8):1143–50.
28. Lee YH, Huang WC, Hsieh MS. CTNNB1 mutations in basal cell adenoma of the salivary gland. J Formos Med Assoc. 2018;117(10):894–901.
29. Sato M, Yamamoto H, Hatanaka Y, Nishijima T, Jiromaru R, Yasumatsu R, et al. Wnt/beta-catenin signal alteration and its diagnostic utility in basal cell adenoma and histologically similar tumors of the salivary gland. Pathol Res Pract. 2018;214(4):586–92.
30. Wilson TC, Ma D, Tilak A, Tesdahl B, Robinson RA. Next-generation sequencing in salivary gland basal cell adenocarcinoma and basal cell adenoma. Head Neck Pathol. 2016;10(4):494–500.
31. Chiosea SI, Miller M, Seethala RR. HRAS mutations in epithelial-myoepithelial carcinoma. Head Neck Pathol. 2014;8(2):146–50.
32. Cros J, Sbidian E, Hans S, Roussel H, Scotte F, Tartour E, et al. Expression and mutational status of treatment-relevant targets and key oncogenes in 123 malignant salivary gland tumours. Ann Oncol. 2013;24(10):2624–9.
33. El Hallani S, Udager AM, Bell D, Fonseca I, Thompson LDR, Assaad A, et al. Epithelial-myoepithelial carcinoma: frequent morphologic and molecular evidence of preexisting pleomorphic adenoma, common HRAS mutations in PLAG1-intact and HMGA2-intact cases, and occasional TP53, FBXW7, and SMARCB1 alterations in high-grade cases. Am J Surg Pathol. 2018;42(1):18–27.
34. Bishop JA, Gagan J, Baumhoer D, McLean-Holden AL, Oliai BR, Couce M, et al. Sclerosing polycystic "adenosis" of salivary glands: a neoplasm characterized by PI3K pathway alterations more correctly named sclerosing polycystic adenoma. Head Neck Pathol. 2020;14(3):630–6.
35. Chiosea SI, Williams L, Griffith CC, Thompson LD, Weinreb I, Bauman JE, et al. Molecular characterization of apocrine salivary duct carcinoma. Am J Surg Pathol. 2015;39(6):744–52.
36. Dalin MG, Desrichard A, Katabi N, Makarov V, Walsh LA, Lee KW, et al. Comprehensive molecular characterization of salivary duct carcinoma reveals actionable targets and similarity to apocrine breast cancer. Clin Cancer Res. 2016;22(18):4623–33.
37. Bishop JA, Gagan J, Krane JF, Jo VY. Low-grade apocrine intraductal carcinoma: expanding the morphologic and molecular spectrum of an enigmatic salivary gland tumor. Head Neck Pathol. 2020. https://doi.org/10.1007/s12105-020-01128-0.